BIOGENESIS FACTOR REQUIRED FOR ATP SYNTHASE 3 Facilitates Assembly of the Chloroplast ATP Synthase Complex[1]

Lin Zhang, Zhikun Duan, Jiao Zhang, and Lianwei Peng*

Key Laboratory of Photobiology, CAS Center for Excellence in Molecular Plant Sciences, Institute of Botany, Chinese Academy of Sciences, Beijing 100093, China (L.Z., Z.D., J.Z., L.P.); and University of Chinese Academy of Sciences, Beijing 100049, China (L.Z., Z.D.)

Thylakoid membrane-localized chloroplast ATP synthases use the proton motive force generated by photosynthetic electron transport to produce ATP from ADP. Although it is well known that the chloroplast ATP synthase is composed of more than 20 proteins with $\alpha_3\beta_3\gamma_1\varepsilon_1\delta_1 I_1 II_1 III_{14} IV_1$ stoichiometry, its biogenesis process is currently unclear. To unravel the molecular mechanisms underlying the biogenesis of chloroplast ATP synthase, we performed extensive screening for isolating ATP synthase mutants in Arabidopsis (*Arabidopsis thaliana*). In the recently identified *bfa3* (*biogenesis factors required for ATP synthase 3*) mutant, the levels of chloroplast ATP synthase subunits were reduced to approximately 25% of wild-type levels. In vivo labeling analysis showed that assembly of the CF_1 component of chloroplast ATP synthase was less efficient in *bfa3* than in the wild type, indicating that BFA3 is required for CF_1 assembly. *BFA3* encodes a chloroplast stromal protein that is conserved in higher plants, green algae, and a few species of other eukaryotic algae, and specifically interacts with the $CF_1\beta$ subunit. The BFA3 binding site was mapped to a region in the catalytic site of $CF_1\beta$. Several residues highly conserved in eukaryotic $CF_1\beta$ are crucial for the BFA3–$CF_1\beta$ interaction, suggesting a coevolutionary relationship between BFA3 and $CF_1\beta$. BFA3 appears to function as a molecular chaperone that transiently associates with unassembled $CF_1\beta$ at its catalytic site and facilitates subsequent association with $CF_1\alpha$ during assembly of the CF_1 subcomplex of chloroplast ATP synthase.

Biosynthesis of ATP by F-type ATP synthases occurs ubiquitously in energy-transducing membranes, providing the main ATP source that drives numerous biochemical reactions in all living cells (Yoshida et al., 2001). In chloroplasts, ATP synthase is located in the thylakoid membrane and comprises two major structural subcomplexes, CF_1 and CF_0 (von Ballmoos et al., 2009; Junge and Nelson, 2015). The CF_1 subcomplex is composed of five different subunits with a stoichiometry of $\alpha_3\beta_3\gamma_1\delta_1\varepsilon_1$, whereas the CF_0 subcomplex is comprised of four different subunits with a stoichiometry of $I_1 II_1 III_{14} IV_1$ (Groth and Pohl, 2001; Vollmar et al., 2009). The α- and β-subunits are arranged alternately to form a spherical $\alpha_3\beta_3$ hexamer. Three catalytic sites (CSs) and three noncatalytic regulatory sites (NCSs) for reversible ATP biosynthesis are located at the interfaces of the α/β subunits. The $\alpha_3\beta_3$ hexamer is fixed by the "stator" embedded in the thylakoid membrane, which includes the $CF_1\delta$ subunit and CF_0 subunits I, II, and IV (Weber, 2007). An elongated α-helical coiled-coil domain of the γ-subunit is inserted into the $\alpha_3\beta_3$ hexamer. Together with the $CF_1\varepsilon$ subunit, $CF_1\gamma$ interacts with the *c*-ring (III_{14}) of the CF_0 subcomplex to form the "rotor." When ATP synthase is activated, efflux of protons drives the rotation of the rotor, and rotation of the γ-subunit inside the $\alpha_3\beta_3$ hexagon induces conformational changes in the $\alpha_3\beta_3$ hexamer, resulting in the biosynthesis and release of ATP (Junge and Nelson, 2015).

Despite our advanced knowledge of the working mechanisms and structure of chloroplast ATP synthase, little is known about the assembly process of this intricate complex, especially on the CF_1 module. To date, only three assembly factors, Alb4, PAB, and CGL160, were shown to be involved in the assembly of chloroplast ATP synthase (Benz et al., 2009; Rühle et al., 2014; Fristedt et al., 2015; Mao et al., 2015). Alb4 is a YidC/Oxa1/Alb3 family protein. It has been shown that Alb4 physically interacts with the $CF_1\beta$ and CF_0II subunits and promotes the assembly of CF_1 during its attachment to CF_0 in the thylakoid membrane (Benz et al., 2009). Arabidopsis (*Arabidopsis thaliana*) CGL160, a homolog of prokaryotic Atp1/UncI proteins, is thought to facilitate *c*-ring formation via interaction with the CF_0II and CF_0III subunits (Rühle et al., 2014). By

[1] This work was financially supported by the National Natural Science Funds for Outstanding Youth (31322007) and the Hundred Talents Program of the Chinese Academy of Sciences.

* Address correspondence to penglianwei@ibcas.ac.cn.

The author responsible for distribution of materials integral to the findings presented in this article in accordance with the policy described in the Instructions for Authors (www.plantphysiol.org) is: Lianwei Peng (penglianwei@ibcas.ac.cn).

A nucleus-encoded factor is involved in the assembly of the chloroplast ATP synthase via a specific interaction with the $CF_1\beta$ subunit.

L.Z. and L.P. conceived the study and designed the experiments; L.Z., Z.D., and J.Z. performed the experiments and analyzed the data; L.Z. and J.Z. produced the figures; and L.P. supervised the whole study and wrote the paper together with L.Z.

www.plantphysiol.org/cgi/doi/10.1104/pp.16.00248

contrast, stromal protein PAB specifically interacts with the γ-subunit and facilitates the assembly of the γ-subunit into the $\alpha_3\beta_3$ hexamer (Mao et al., 2015).

In vitro reconstitution and mutant characterization in *Chlamydomonas* and Arabidopsis suggested that the first and key step of CF_1 assembly is the formation of the α/β heterodimer (Chen and Jagendorf, 1994). In parallel, the nucleus-encoded γ-subunit is imported into the chloroplast and folded by the Cpn60 complex (Mao et al., 2015). With the help of the molecular chaperone PAB, the folded γ-subunit may interact with the α/β heterodimer and direct the hexamerization of $\alpha_3\beta_3$, leading to the formation of the $\alpha_3\beta_3\gamma$ subcomplex (Wollman et al., 1999; Choquet and Vallon, 2000; Hippler et al., 2002; Mao et al., 2015). An alternate hypothesis is that the $\alpha_3\beta_3$ hexamer is assembled from α/β heterodimers, and the folded γ-subunit is then inserted into the hexamer to form the active CF_1 module (Strotmann et al., 1998; Rühle and Leister, 2015). In both assembly models, formation of the α/β heterodimer is a key step and a prerequisite for subsequent assembly with other subunits. However, it remains largely unknown how the α/β heterodimer is formed in chloroplasts. In mitochondria, formation of the α/β heterodimer is thought to be facilitated by two assembly factors: Atp11p and Atp12p (Ackerman and Tzagoloff, 2005; Rak et al., 2011). Whereas Atp11p specifically interacts with unassembled β-subunit at the surface that forms the CS with an adjacent α-subunit, Atp12p binds to the α-subunit at the surface that forms the NCS with the β-subunit (Wang et al., 2000; Wang and Ackerman, 2000). The regions harboring the CSs and NCSs at the α/β surfaces display hydrophobic properties, and formation of the Atp11p-β and Atp12p-α intermediate is believed to prevent aggregation of monomeric subunits. However, an assembly factor that specifically interacts with α- or β-subunits in chloroplasts (similar to Atp11p and Atp12p in mitochondria) has not been identified.

To gain insight into the processes involved in chloroplast ATP synthase assembly, we performed extensive screening to isolate ATP synthase mutants. We identified several Arabidopsis mutants with low levels of chloroplast ATP synthase, which we designated *bfa* mutants (as the mutated genes encode biogenesis factors required for ATP synthase; see "Discussion" for more detail). Characterization of the *bfa3* mutants identified a novel assembly factor, BFA3, which specifically interacts with the $CF_1\beta$ subunit and facilitates assembly of the CF_1 subcomplex of chloroplast ATP synthase.

RESULTS

Isolation of the *bfa3* Mutant

Nonphotochemical quenching (NPQ) is an efficient photoprotective mechanism in which absorbed excess light energy is safely dissipated as heat. The main component of NPQ, qE, is strictly triggered and controlled by lumen acidification (Niyogi, 1999). During the dark-to-light (80 μmol photons s^{-1} m^{-2}) transition, NPQ was transiently induced to 0.8 within 1 min in wild-type plants (Fig. 1, A and B); this phenomenon is closely related to acidification of the thylakoid lumen, which is likely caused by the activation of cyclic electron transport around PSI (Munekage et al., 2002; DalCorso et al., 2008). Due to the activation of ATP synthase upon illumination, proton efflux from the thylakoid lumen occurs via chloroplast ATP synthase, and NPQ is rapidly relaxed within 2 min postinduction in the wild type (Fig. 1, A and B). However, if ATP synthase activity is reduced, proton efflux via ATP synthase would be insufficient, resulting in the accumulation of high levels of protons in the lumen and, consequently, preventing the relaxation of NPQ. Thus, NPQ levels after exposure to actinic light for 2 min can be used as an evaluation parameter for isolating mutants with low ATP synthase activity. Based on this hypothesis, we screened a large collection of pSKI015 T-DNA insertion Arabidopsis lines. Using this process, we isolated the *bfa3-3* line.

Thermal asymmetric interlaced polymerase chain reaction (TAIL-PCR) was performed to unravel the genetic basis of the *bfa3-3* mutant. The pSKI015 T-DNA was inserted in the tenth intron of *At2g21385* in this mutant (Fig. 1C). To confirm that the disruption of *At2g21385* is responsible for the observed phenotype, *bfa3-1* (SALK_019326) and *bfa3-2* (SALK_006444C) were obtained from the European Arabidopsis Stock Centre (NASC; Fig. 1C). No transcripts were detected after 35 rounds of reverse transcription (RT)-PCR for all three alleles (Fig. 1D), indicating that they are knockout alleles. All three alleles had the same phenotypes (Fig. 1). In addition, we introduced the wild-type *At2g21385* sequence into *bfa3-1*, which fully complemented the mutant phenotypes (Fig. 1A), indicating that disruption of *At2g21385* is responsible for the phenotypes of the *bfa3* mutants.

Phenotype of the *bfa3* Mutant

When grown on soil under low light conditions (50 μmol photons m^{-2} s^{-1}), the seedling size of *bfa3* was reduced to approximately 75% of wild type at 30 d after germination (Fig. 1, A and E). As expected, in both wild-type and *BFA3*-complemented plants, NPQ was transiently induced to approximately 0.8 within 1 min of exposure to light and relaxed to approximately 0.4 during subsequent illumination (Fig. 1, A and B). In the *bfa3* mutants, however, NPQ was more rapidly induced to 1.0 within 30 s of illumination. Although slight relaxation was observed in *bfa3* after 2 min illumination, NPQ was maintained at a high level of approximately 1.2 (Fig. 1, A and B). To confirm that the high NPQ observed during the dark-to-light transition is caused by low ATP synthase activity in *bfa3*, we analyzed the light intensity dependence of the conductivity of the thylakoid to protons, g_H^+ (Fig. 1F). The electrochromic shift (ECS) signal reflects changes in the electric field across the thylakoid membrane, and the total relaxation

of the ECS signal during a light-dark transition represents the light-induced proton motive force (pmf; Bailleul et al., 2010). Due to the absence of photosynthetic electron transport in darkness, the initial ECS decay upon switching off actinic light mainly reflects proton efflux through ATP synthase; therefore, the H^+ conductivity of ATP synthase can be estimated based on the kinetics of the initial ECS decay (Cruz et al., 2001). In both mutants, g_{H^+} was consistently reduced to approximately 50% of wild-type levels at all light intensities investigated, confirming that ATP synthase activity is reduced in *bfa3* (Fig. 1F).

The pmf can be partitioned into two components, ΔpH and $\Delta\Psi$, both of which are thermodynamically equivalent when driving ATP synthase. We found that the total pmf and its two components were significantly higher in *bfa3* than in the wild-type under both low-light (89 μmol photons m^{-2} s^{-1}; Figure 2A) and high-light (754 μmol photons m^{-2} s^{-1}; Figure 2B) intensities, indicating a higher proton accumulation level in the thylakoid lumen of *bfa3*. Consistent with the observation that high levels of protons accumulated in the *bfa3* lumen, the steady-state NPQ in *bfa3* was higher than that in the wild type at light intensities >100 μmol photons m^{-2} s^{-1} (Fig. 2C).

Light intensity dependence of the electron transport rate through PSII (ETR) was analyzed. Compared with the wild type, lower ETR levels were observed in *bfa3* at light intensities >200 μmol photons m^{-2} s^{-1} (Fig. 2D), indicating that the linear electron transport rates were strongly depressed. We also determined the light intensity dependence of 1-qL, which represents the reduction state of plastoquinone at the PSII acceptor side, as well as the light intensity-dependent oxidation of the donor side of PSI. Higher 1-qL levels were observed in *bfa3* at light intensities of >200 μmol photons m^{-2} s^{-1}, indicating that the PSII acceptor side is much more reduced in *bfa3* than in the wild type (Fig. 2E). Furthermore, the PSI donor side was more oxidized than the wild type under all light conditions (Fig. 2F). These results indicate that photosynthetic linear electron transport is inhibited between PSII and PSI in *bfa3*. Similar photosynthetic properties were observed in tobacco (*Nicotiana tabacum*) plants with low accumulation of chloroplast ATP synthase, in which linear electron transport is strongly inhibited at the cytochrome b_6f (Cyt b_6f) complex via the photosynthetic control mechanism (Foyer et al., 1990; Kanazawa and Kramer, 2002; Rott et al., 2011).

Accumulation of Chloroplast ATP Synthase Is Drastically Reduced in *bfa3*

We monitored the abundance of the major thylakoid protein complexes by immunoblot analysis (Fig. 3). In all three *bfa3* mutants, the levels of CF_1 subunits (α, β, γ, ε, and δ) and two subunits in the CF_0 segment (CF_0I and CF_0II) were reduced to approximately 25% of wild-type levels (Fig. 3A). By contrast, identical levels of PSII (D1 and LHCII), PSI (PsaA), and Cyt b_6f (Cyt *f*) complexes were observed between *bfa3* and wild-type plants (Fig. 3A). These results indicate that BFA3 is specifically required for the accumulation of chloroplast ATP synthase. To further investigate the role of BFA3 in ATP synthase biogenesis, thylakoid membrane was solubilized in 1% *n*-dodecyl-β-D-maltoside and the protein complexes were separated by blue native (BN)-PAGE. As shown in Figure 3B, formation of most thylakoid protein complexes, such as the NDH-PSI supercomplex, PSII supercomplexes, PSI monomer, and LHCII trimer, is unaffected in the mutants (Fig. 3B). Subsequent two-dimensional (2D) SDS-PAGE analysis showed that the majority of α-, β-, and γ-subunits were detected in the intact CF_0-CF_1 ATP synthase and CF_1 subcomplex in wild-type plants (Fig. 3C). A putative complex containing the β-subunit was also found in the wild-type thylakoids (Fig. 3C). In the *bfa3* mutants, the levels of α-, β-, and γ-subunits were significantly reduced but were mainly detected in intact ATP synthase, as in wild-type plants (Fig. 3C). These results indicate that the residual subunits in *bfa3* form functional ATP synthase, which explains why approximately 50% ATP synthase activity remained in *bfa3* (Fig. 1).

Assembly of Chloroplast ATP Synthase in Thylakoids Is Impaired in *bfa3*

In chloroplasts, ATP synthase genes are present in two gene clusters, *atpI/H/F/A* and *atpB/E*, both of which are processed into several different transcripts (Supplemental Fig. S1, A and B; Malik Ghulam et al., 2012). One possible explanation for the reduced ATP synthase level in *bfa3* is that the maturation or translation initiation of these genes is disrupted. To test this possibility, RNA gel blot and polysome association analyses were performed to investigate the expression of the chloroplast-encoded ATP synthase genes. No drastic alterations in the patterns of these genes were found in *bfa3* (Supplemental Fig. S1C). Although *atpH/F* transcript levels were reduced to approximately one-half of wild-type levels in *bfa3*, their association with the polysome was unaffected (Supplemental Fig. S1E), suggesting efficient translation of *atpH/F*. By contrast, levels of *atpB/E* transcripts were significantly higher in *bfa3* than in wild-type plants (Supplemental Fig. S1D). Furthermore, we did not observe drastic changes in the association of polysomes with *atpB/E* transcripts (Supplemental Fig. S1E), suggesting an efficient synthesis of the $CF_1\beta/\varepsilon$ subunits. Thus, it is likely that the drastic reduction in chloroplast ATP synthase levels in *bfa3* is due to defects in posttranslational steps during its biogenesis.

We investigated the rates of de novo chloroplast protein biosynthesis in *bfa3* via in vivo pulse labeling experiments. After incubation with cycloheximide, which inhibits the translation of nucleus-encoded proteins, seedling leaves were labeled with [^{35}S]-Met for 20 min. Thylakoid protein was then isolated and newly synthesized plastid-encoded proteins were visualized by autoradiography (Fig. 4A). In the two *bfa3* mutants,

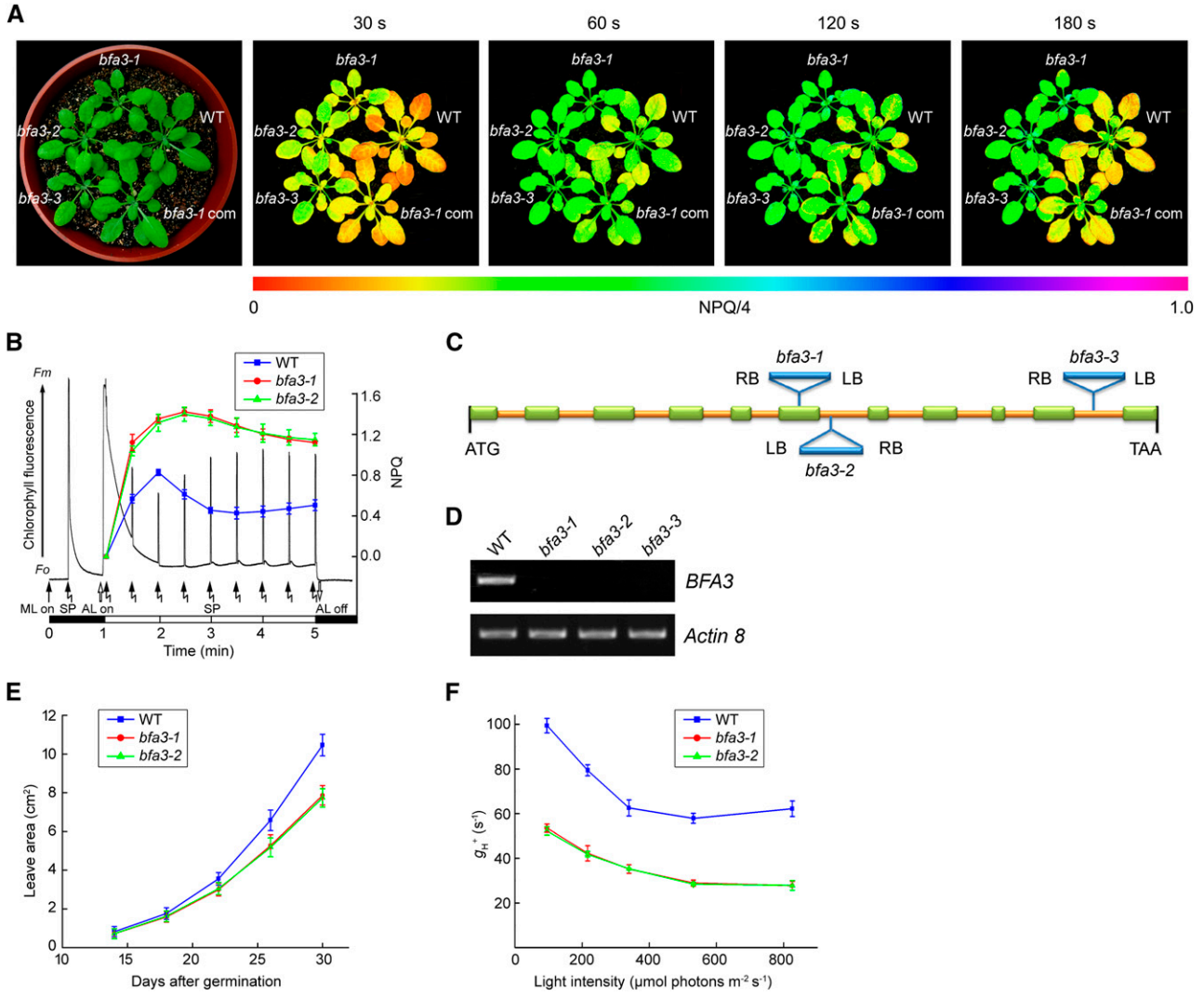

Figure 1. Characterization of *bfa3* mutants. A, Phenotype of 4-week-old *bfa3* mutants. Images of NPQ were captured upon illumination for 30 s to 180 s (right). Signal intensities for NPQ/4 are indicated according to the color scale (from 0 to 1.0) at the bottom. WT, wild type; *bfa3-1* com, *bfa3-1* mutant complemented by introducing the genomic sequence of *BFA3*. B, Time course of NPQ induction. The black line represents a typical trace of chlorophyll fluorescence in WT. Induction of NPQ was monitored for 4 min at 80 μmol photons m^{-2} s^{-1} light intensity (colored lines). F_0, minimal chlorophyll fluorescence; *Fm*, maximum chlorophyll fluorescence; ML, measuring light; SP, saturating light pulse. The black and white bars indicate darkness and actinic light (AL) illumination, respectively. Data are presented as the means ± SD (n = 3). C, Schematic representation of *BFA3* in Arabidopsis. T-DNA insertion positions are indicated. Exons are shown as green rectangles and introns as yellow lines. D, RT-PCR analysis of *BFA3* transcript accumulation in *bfa3*. *Actin8* was used as a control. E, Growth rates of the *bfa3* mutants compared with wild-type plants. Values are means ± SD (n = 3). (F) Light intensity dependence of H^+ conductivity through ATP synthase (g_H^+).

the rates of biosynthesis of the $CF_1\alpha$ and $CF_1\beta$ subunits of ATP synthase, as well as the subunits of PSI (PsaA/B) and PSII (CP47, CP43 and D1/D2), were almost identical to those in the wild type (Fig. 4A). After 20 min of pulse labeling, the newly synthesized proteins were further chased for various periods of time with cold Met (Fig. 4B). In the wild type, the levels of newly synthesized ATP synthase $CF_1\alpha/\beta$ subunits were unaltered during the 2-h chase. However, the turnover rates of ATP synthase $CF_1\alpha/\beta$ subunits were significantly higher in the *bfa3* mutants than in the wild type (Fig. 4B), indicating that the newly synthesized $CF_1\alpha/\beta$ subunits were unstable in *bfa3*, although they could be synthesized at normal rates as in the wild type (Fig. 4A).

Assembly kinetics of chloroplast ATP synthase was further investigated via protein pulse labeling and chasing in combination with 2D BN/SDS-PAGE. After pulse labeling for 20 min, newly synthesized $CF_1\alpha/\beta$ subunits were detected in intact ATP synthase and CF_1 subcomplex in the wild type (chase time: 0 min; Figure 4C). The putative complex containing $CF_1\beta$ was also detected (Fig. 4C). During subsequent chasing for 15,

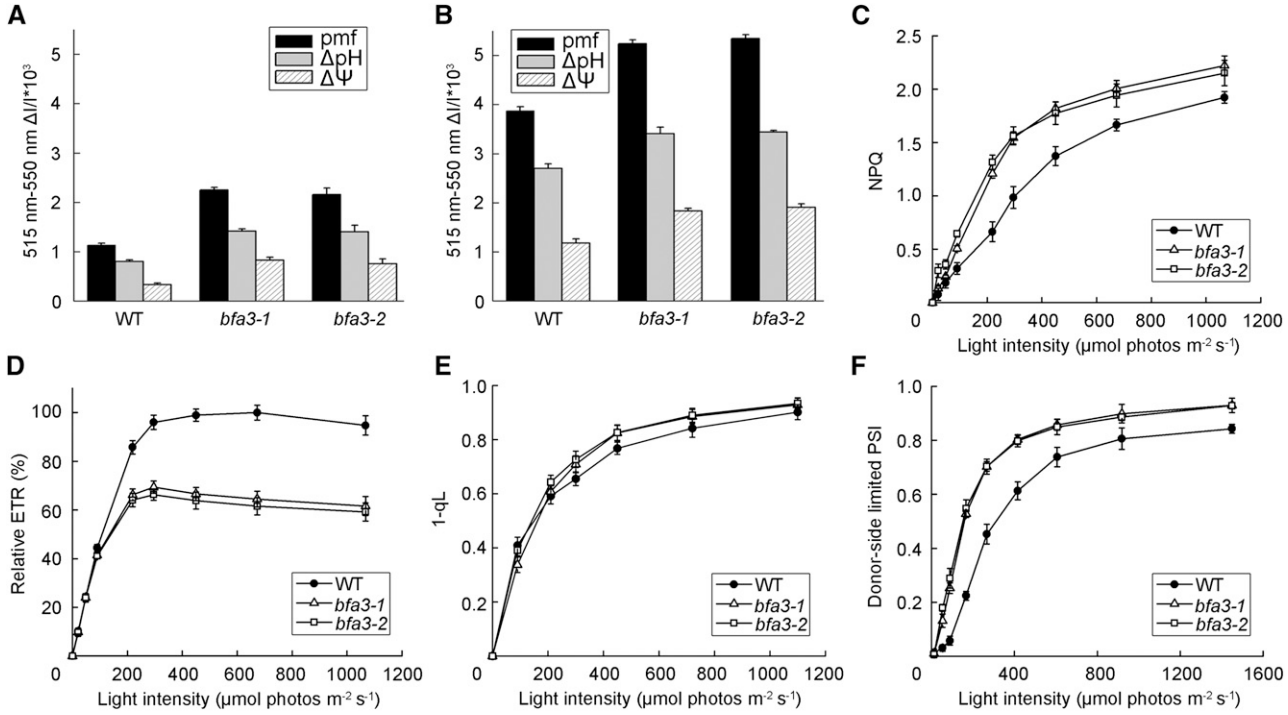

Figure 2. Photosynthetic properties of *bfa3* and wild-type plants. A and B, pmf across the thylakoid membrane. The pmf was determined by the slowly relaxing phase of the ECS signal after illuminating the leaves with 89 (A) and 754 (B) μmol photons m^{-2} s^{-1} light for 10 min. The pmf was further partitioned into the pH gradient component (ΔpH) and the electric field component ($\Delta\Psi$). C–F, Light intensity dependence of NPQ (C), relative ETR (D), 1-qL (E), and oxidation of the donor side of PSI (F). ETR is presented as the maximum value of Φ_{PSII} × light intensity in the wild type (100%). All values are means ± SD of three independent plants (n = 3).

30, and 60 min, the relative abundance of intact ATP synthase and CF_0 subcomplex as well as of the putative complex containing $CF_1\beta$ progressively increased in the wild type (Fig. 4C). However, in the two *bfa3* mutants, the newly synthesized ATP synthase $CF_1\alpha/\beta$ subunits were not detected in any of the three complexes via 2D BN/SDS-PAGE after pulse labeling and subsequent chasing (Fig. 4C), indicating that the assembly of ATP synthase is strongly impaired in the *bfa3* mutants.

Assembly of the CF_1 subcomplex Is Impaired in the Chloroplast Stroma of *bfa3*

The catalytic CF_1 domain of ATP synthase protrudes into the chloroplast stroma and is composed of five different subunits ($CF_1\alpha$ to $CF_1\varepsilon$). Interestingly, in addition to the thylakoid membrane, substantial amounts of CF_1 subunits (approximately one-eighth to one-fourth of total ATP synthase in thylakoids) were also detected in the chloroplast stroma (Fig. 5A). Even though ATP synthase levels in *bfa3* thylakoids were only approximately one-fourth of those in the wild type (Fig. 3A), CF_1 subunit levels in the stroma were slightly lower in *bfa3* than in the wild type (Fig. 5B). Clear-native (CN)-PAGE and immunoblot analysis showed that all of the stroma-localized CF_1 subunits form an intact CF_1 subcomplex (Fig. 5C).

To investigate whether the stroma-localized CF_1 subcomplex is synthesized and assembled in the chloroplast stroma, total soluble protein was extracted from leaves and separated by SDS-PAGE after pulse labeling with [^{35}S]-Met and chasing in the presence of cycloheximide (Fig. 6A). The large subunit of the Rubisco complex, RbcL, was predominantly labeled in the chloroplast stroma in both the wild type and the *bfa3* mutants (Fig. 6A). The results show that the $CF_1\alpha$ subunit is synthesized in the chloroplast stroma and its synthesis rate is unaffected in the *bfa3* mutants compared with wild-type plants (20-min pulse labeling; lanes indicated as 0 in Figure 6A). The $CF_1\beta$ signal was masked by that of RbcL due to their similar molecular masses. After chasing for as long as 2 h, newly synthesized $CF_1\alpha$ was not degraded in the chloroplast stroma of *bfa3* or wild-type plants (Fig. 6A), indicating that $CF_1\alpha$ is highly stable in the chloroplast stroma after synthesis.

In the stroma of wild-type plants, newly synthesized $CF_1\alpha/\beta$ subunits were efficiently assembled into the CF_1 subcomplex after 20 min of pulse labeling (lanes indicated as 0 in Figure 6B), and the level of CF_1 subcomplex progressively increased during subsequent 30- and 60-min chases (Fig. 6, B and C), indicating that the CF_1 subcomplex was also actively assembled in the chloroplast stroma. However, the level of newly assembled CF_1 subcomplex was significantly reduced in

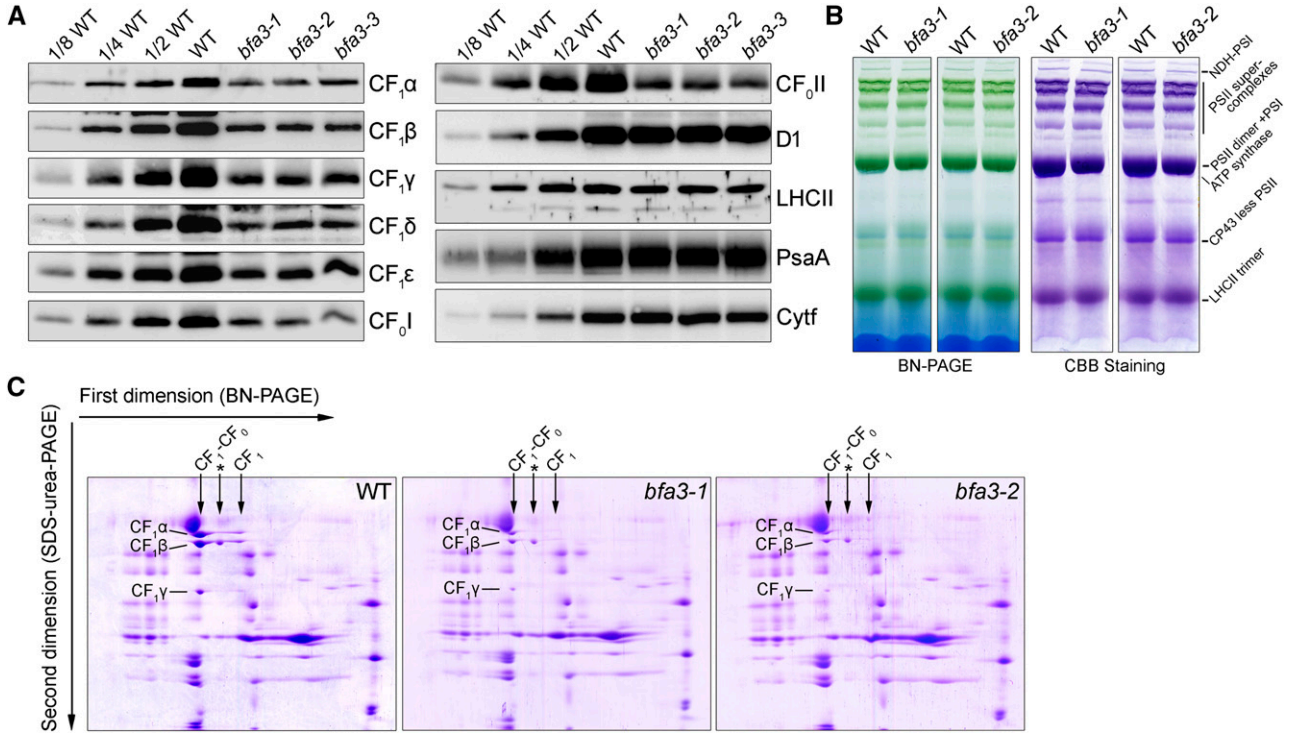

Figure 3. Analysis of thylakoid protein complexes from *bfa3* and wild-type plants. A, Immunodetection of thylakoid proteins from *bfa3* and WT plants. Thylakoid proteins were loaded on an equal chlorophyll basis. B, BN gel analysis of thylakoid membrane protein complexes. The BN gel (left) was further stained with Coomassie Brilliant Blue (CBB; right). NDH-PSI, NDH-PSI supercomplex. C, 2D BN/SDS-PAGE separation of thylakoid protein complexes. Complexes separated by BN-PAGE (B) were resolved into their constituent subunits by SDS-urea-PAGE. Proteins were stained with CBB; the identities of relevant proteins are indicated. The position of intact chloroplast ATP synthases (CF_1-CF_0) and the CF_1 subcomplex (CF_1) in the first dimension are indicated with arrows. The complex between the CF_1-CF_0 ATP synthase and CF_1 subcomplex (marked with an asterisk) is a putative complex containing the β-subunit.

bfa3 stroma compared to the wild type (Fig. 6, B and C), implying that the assembly of the CF_1 subcomplex in the chloroplast stroma is impaired in *bfa3*.

In conclusion, these results demonstrate that assembly of the CF_1 subcomplex of chloroplast ATP synthase is less efficient in *bfa3* than in wild-type plants, indicating that the protein encoded by the mutated gene in *bfa3* is involved in the assembly of the CF_1 subcomplex.

BFA3 Is a Chloroplast Stromal Protein

BFA3 encodes a 330-amino acid protein with no known function. Orthologs of BFA3 are present in photosynthetic Viridiplantae (land plants and green algae) and a few species of other eukaryotic algae, but no homolog was found in prokaryotic algae (Fig. 7A; Supplemental Fig. S2; Supplemental Table S1). The first 47 amino acids of AtBFA3 are predicted to comprise a plastid-targeting signal (Supplemental Fig. S2), suggesting chloroplast localization of BFA3. To confirm this hypothesis, we transiently transformed Arabidopsis protoplasts with a *BFA3-GFP* (GFP) fusion construct. Confocal laser scanning microscopy confirmed that BFA3 is specifically localized to the chloroplast (Fig. 7B). To determine the localization of BFA3 more precisely, we raised polyclonal antibodies against recombinant BFA3 protein and used them to probe membrane and stromal fractions isolated from intact chloroplasts from the wild type and the three *bfa3* mutants. A protein with a molecular mass of slightly less than 35 kD was detected in the stromal fraction from wild-type plants (the calculated molecular mass of mature BFA3 is 31.5 kD; Figure 7C) but was absent in the three *bfa3* mutants and in the membrane fraction of wild-type plants (Fig. 7C), indicating that BFA3 is a chloroplast stromal protein. This conclusion is consistent with the observation that no transmembrane domain was predicted by the TMHMM program (http://www.cbs.dtu.dk/severces/TMHMM-2.0/).

BFA3 Specifically Interacts with the β-Subunit of Chloroplast ATP Synthase

Since our results indicate that BFA3 is involved in the assembly of the CF_1 subcomplex of chloroplast ATP synthase, we investigated whether BFA3 interacts with subunits of the ATP synthase complex. To investigate whether BFA3 interacts with other protein(s) and forms

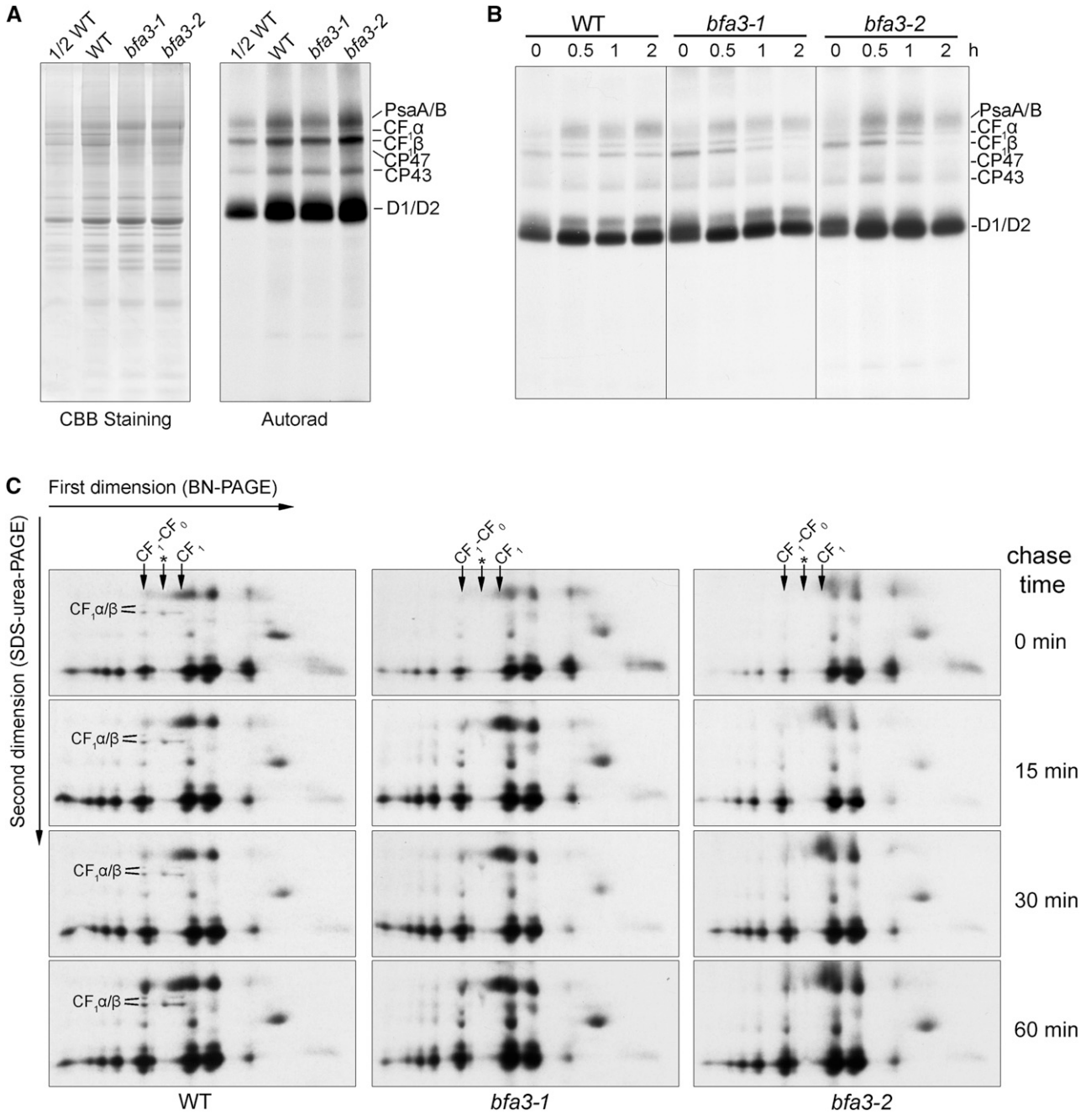

Figure 4. In vivo protein labeling of plastid-encoded thylakoid membrane proteins. A, Pulse labeling of thylakoid proteins of *bfa3* and WT plants. After pulse labeling with [^{35}S]-Met for 20 min, thylakoid proteins were separated by SDS-urea-PAGE (left), and the labeled proteins were visualized by autoradiography (right). B, Pulse-chase labeling of thylakoid membrane proteins. After pulse labeling with [^{35}S]-Met for 20 min as in (A), the leaves were incubated with excess cold Met for an additional 0.5, 1, and 2 h. Labeled proteins were visualized by subsequent SDS-urea-PAGE and autoradiography. C, Assembly kinetics of the thylakoid protein complexes. After pulse-chase labeling as in B, except that the leaves were chased for 15, 30, and 60 min, and thylakoid protein complexes were separated by 2D BN/SDS-PAGE. The labeled proteins were visualized by autoradiography. $CF_1\alpha/\beta$ subunits are indicated as in Figure 3C. The position of intact chloroplast ATP synthases (CF_1-CF_0) and CF_1 subcomplex (CF_1) in the first dimension are indicated with arrows. The complex between the CF_1-CF_0 ATP synthase and CF_1 subcomplex (marked with an asterisk) is a putative complex containing the β-subunit.

a complex in the stroma, we separated chloroplast stromal protein complexes isolated from wild-type plants by Suc density gradient centrifugation. Immunoblot analysis showed that CF_1 subunits comigrated, forming the CF_1 subcomplex of ATP synthase (Supplemental Fig. S3), which is consistent with the results obtained by CN-PAGE (Fig. 5C). However, BFA3 appeared to be present in free form (Supplemental

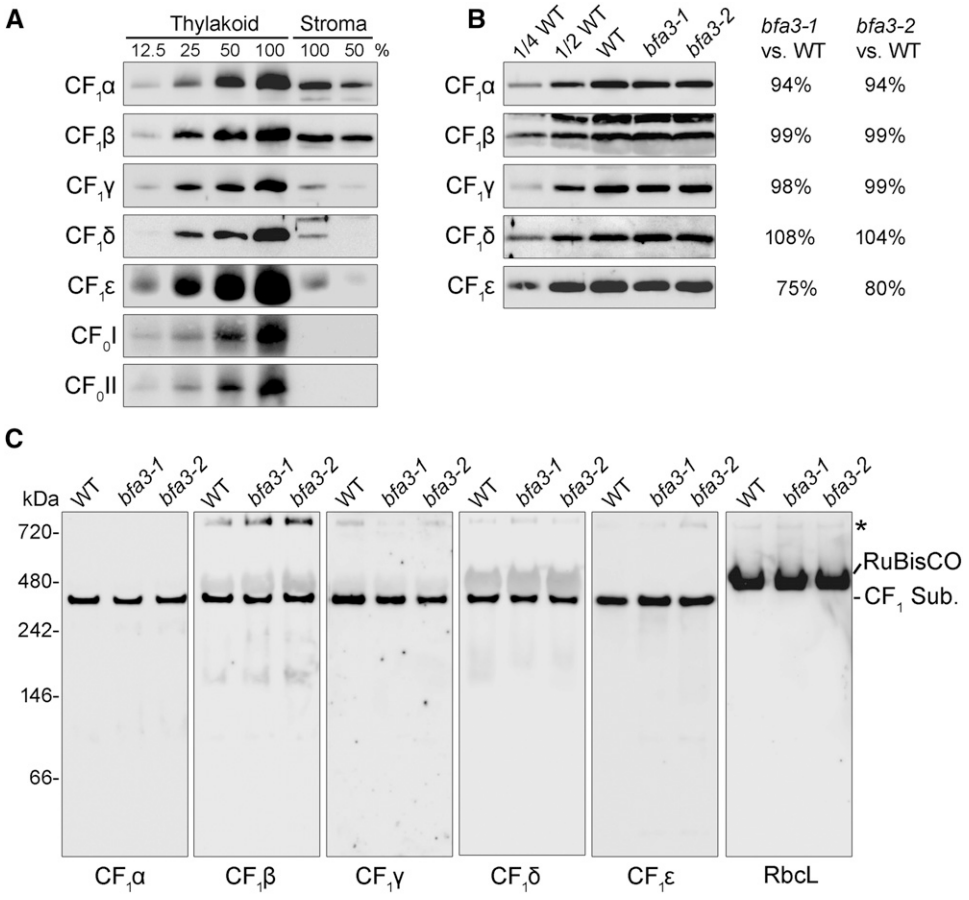

Figure 5. Analysis of the stromal protein from *bfa3* and wild-type plants. A, Immunodetection of ATP synthase subunits isolated from the thylakoid and stroma of WT plants. Intact chloroplasts of WT plants were fractionated into thylakoid membrane and stromal fractions. Stoichiometric amounts of thylakoid and stromal fractions were fractionated by SDS-urea-PAGE and detected with the specific antibodies indicated. A dilution series of thylakoid and stromal protein is shown. B, Immunodetection of ATP synthase subunits isolated from the stromal fractions of WT and *bfa3* plants. Samples were loaded on an equal protein content basis. Signals of *bfa3* mutants were quantified as percentages of the wild-type signal and are presented on the right. C, CN-PAGE analysis of the CF_1 subcomplex of ATP synthase. Stromal protein complexes isolated from WT and *bfa3* plants were separated by CN-PAGE. After denaturation on a CN-gel, the proteins were transferred onto nitrocellulose membranes and immunodetected with antibodies against subunits of ATP synthase ($CF_1\alpha$-$CF_1\varepsilon$), as well as the large subunit of Rubisco (RbcL). CF_1 Sub., CF_1 subcomplex of chloroplast ATP synthase. The band at the top of the CN-gel (indicated by an asterisk) may represent aggregates of the protein.

Fig. S3), indicating that BFA3 does not form a stable complex with CF_1 in the chloroplast stroma.

To identify the subunit(s) that interact with BFA3, its associated proteins were affinity enriched from *bfa3-1* complemented with BFA3-HA (designated *bfa3*-HA plants) using an anti-hemagglutinin (HA) Affinity Matrix. After cross-linking on the intact chloroplast with the membrane-permeable cross-linker dithiobis (succinimidyl propionate) (DSP), chloroplasts were fractionated into stromal and membrane fractions, which were both used for affinity chromatography. Immunoblot analysis showed that only the $CF_1\beta$ subunit was copurified with BFA3 in both the stromal and thylakoid fractions of the *bfa3*-HA affinity sample (Fig. 8A), indicating a specific interaction between BFA3 and $CF_1\beta$. Without chemical cross-linking, however, no subunits of ATP synthase can be purified with BFA3 (Fig. 8A), suggesting that BFA3 transiently interacts with $CF_1\beta$ during the assembly of the CF_1 subcomplex. Yeast two-hybrid and pull-down analysis further confirmed the specific interaction between BFA3 and $CF_1\beta$ in vivo and in vitro (Fig. 8, B and C; Supplemental Fig. S4).

BFA3 Interacts with $CF_1\beta$ at the CS Site with an Adjacent α-Subunit

To elucidate the function of BFA3, it is important to identify the binding site for BFA3 on the $CF_1\beta$ subunit. Based on the crystal structure of ATP synthase from spinach (*Spinacia oleracea*) chloroplasts, the $CF_1\beta$ subunit can be divided into three domains (Figs. 9A and 10A): an N-terminal domain containing a six-stranded β-barrel

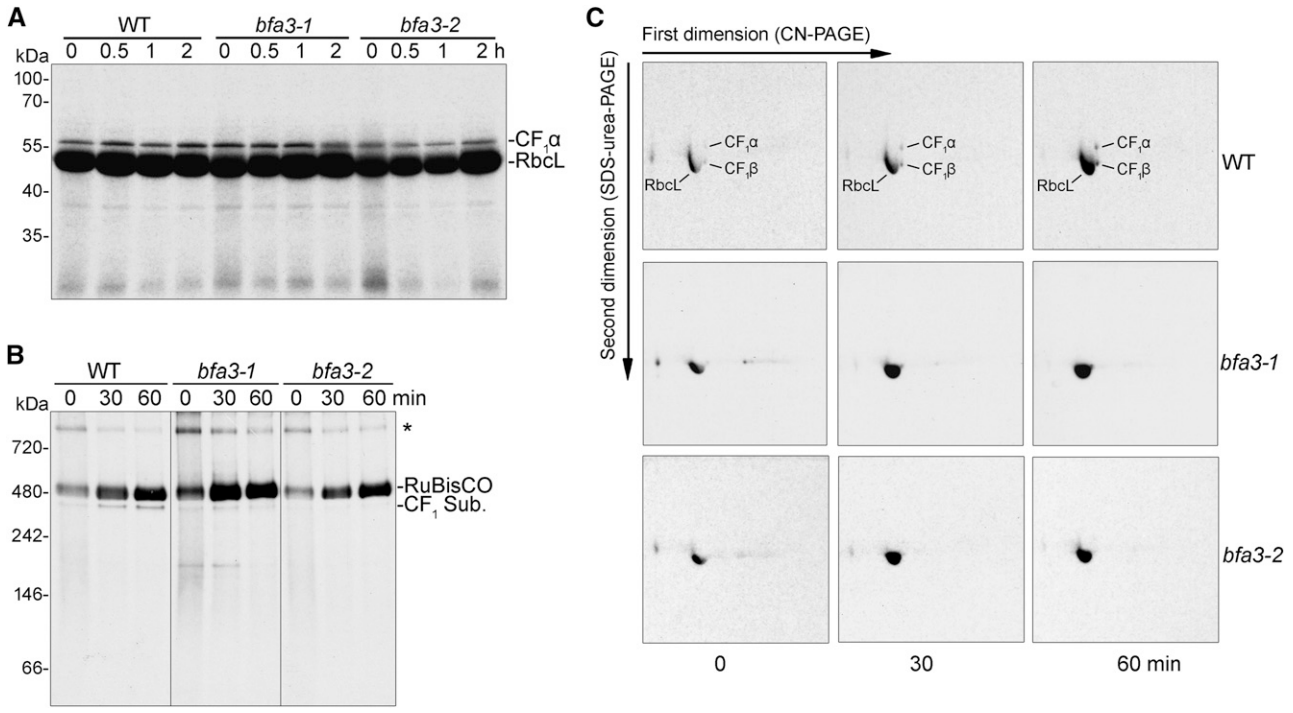

Figure 6. In vivo labeling of plastid-encoded stromal proteins. A, Pulse-chase labeling of the chloroplast stromal proteins. After 20-min pulse labeling (indicated as 0) and chase for 0.5, 1, and 2 h, total soluble proteins were separated by SDS-urea-PAGE and the labeled proteins were visualized by autoradiography. B and C, Pulse-chase labeling of stromal protein complexes. After pulse (indicated as 0) and chase for 30 and 60 min, stromal protein complexes were isolated and separated by CN-PAGE (B) and subsequent 2D/SDS-urea-PAGE (C). The labeled proteins were visualized by autoradiography. CF_1 Sub., CF_1 subcomplex of chloroplast ATP synthase. The band at the top of the CN-gel (indicated by an asterisk) (B) may represent protein aggregates or the chaperonin complex containing unfolded protein.

($CF_1\beta$I), a central domain containing the nucleotide-binding site ($CF_1\beta$II), and a C-terminal α-helical bundle ($CF_1\beta$III; Groth and Pohl, 2001). Yeast two-hybrid analysis showed that BFA3 specifically interacts with the central domain of $CF_1\beta$ ($CF_1\beta$II; Fig. 9B). The $CF_1\beta$ central domain ($CF_1\beta$II) was further divided into three regions: $CF_1\beta$II-1 (Pro-97-Gly-165), a long loop located on the outside surface of the $\alpha_3\beta_3$ hexamer; $CF_1\beta$II-2 (Gly-166-Ile-275), containing three α-helices and four β-strands and forming the CS site with an adjacent $CF_1\alpha$ subunit; and $CF_1\beta$II-3 (Phe-276-Pro-377), which is mainly located inside the $\alpha_3\beta_3$ hexamer and close to the NCS site with another adjacent $CF_1\alpha$ (Figs. 9A and 10A). Only the second region of the $CF_1\beta$ central domain ($CF_1\beta$II-2) was found to interact with BFA3 (Fig. 9B), implying that BFA3 associates with the $CF_1\beta$ subunit at the surface that forms the CS site with an adjacent α-subunit during the assembly of the chloroplast ATP synthase (Fig. 10A).

Several Residues Conserved in $CF_1\beta$ Subunits in Photosynthetic Eukaryotes Are Critical for the Interaction between BFA3 and $CF_1\beta$

No homolog of BFA3 was found in cyanobacteria (Fig. 7A), indicating that assembly of cyanobacterial ATP synthase is independent of BFA3. Consistent with this idea, yeast two-hybrid analysis showed that the interaction between $SynCF_1\beta$ and BFA3 is significantly weaker than that between $AthCF_1\beta$ and BFA3 (Fig. 9, D and E). This result indicates that the $CF_1\beta$ subunit underwent at least a few evolutionary changes from cyanobacteria to photosynthetic eukaryotes and that these changes were beneficial for its binding with BFA3, which occurs in *Chlamydomonas* and land plants. Indeed, protein alignment of the $CF_1\beta$ subunits from cyanobacteria and land plants showed that, although the $CF_1\beta$ subunits are highly conserved, a dozen residues conserved in cyanobacterial $CF_1\beta$ have been replaced by different amino acids that are also conserved in $CF_1\beta$ subunits from land plants as well as *Chlamydomonas* (Fig. 9C; Supplemental Fig. S5). Perhaps these residues, which are highly conserved in $CF_1\beta$ subunits in photosynthetic eukaryotes, are critical for the interaction with BFA3.

To investigate which amino acids are crucial for this interaction, we produced 12 cyanobacterial $SynCF_1\beta$ subunit mutant proteins (designated mβ1–mβ12; Fig. 9A), in which the residues conserved only in cyanobacterial $CF_1\beta$ were converted into the corresponding amino acids of $AthCF_1\beta$ (Fig. 9C; Supplemental Fig. S5). We performed yeast two-hybrid analysis to determine

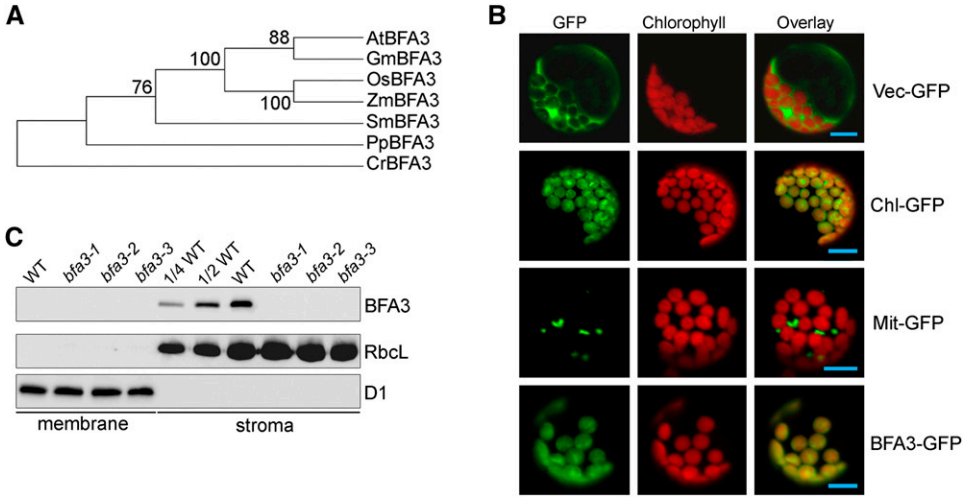

Figure 7. Characterization of BFA3. A, Phylogenetic tree of BFA3 proteins. The sequences were retrieved from GenBank, and evolutionary analyses were conducted in MEGA5 using the neighbor-joining method. B, Transient expression of BFA3-GFP in Arabidopsis protoplasts. Arabidopsis protoplasts were transformed with various vectors and examined by confocal microscopy. Bars = 5 μm. C, Immunodetection of BFA3. Thylakoid and stromal proteins isolated from *bfa3* and WT plants were separated by SDS-urea-PAGE and immunodetected with polyclonal antisera against BFA3. D1 and RbcL were used as fractionation and loading controls.

the relative strength of the interaction between the Syn$CF_1\beta$ mutant proteins and BFA3 by investigating yeast growth rates and alpha-galactosidase activity. Three Syn$CF_1\beta$ mutant proteins (mβ5, mβ8, and mβ9, corresponding to residues 181Leu-182Ile, 217Lys, and 224Glu-228Ala in Ath$CF_1\beta$, respectively) exhibited stronger interactions with BFA3 than did native Syn-$CF_1\beta$ (Fig. 9, D and E), indicating that the amino acids at these three sites are critical for the interaction between $CF_1\beta$ and BFA3. These residues are located in the second region of the $CF_1\beta$ central domain (Fig. 9C), which is consistent with the finding that the second region of this domain ($CF_1\beta$II-2) is the only region of $CF_1\beta$ that interacts with BFA3 (Fig. 9B). To confirm that the residues at these three sites in $CF_1\beta$ are critical for the interaction with BFA3, we converted these residues in Ath$CF_1\beta$ into the corresponding amino acids in Syn-$CF_1\beta$ (mAth$CF_1\beta$589). As expected, mAth$CF_1\beta$589 interacted weakly with BFA3 compared with native Ath$CF_1\beta$ (Fig. 9, F and G). Therefore, amino acids 181Leu-182Ile, 217Lys, and 224Glu-228Ala in Ath$CF_1\beta$ are crucial for the interactions between $CF_1\beta$ and BFA3. Based on the crystal structure of spinach $CF_1\beta$, these residues in mβ5 and mβ8 are predicted to be located close to the nucleotide-binding amino acids in $CF_1\beta$ at the CS surface (Fig. 10A).

DISCUSSION

Identifying and characterizing assembly factors is a key strategy for elucidating the assembly mechanism of multisubunit protein complexes. Due to the highly dynamic regulation of chloroplast ATP synthase activity in the light, even a moderate reduction in ATP synthase content does not significantly reduce its activity (Rott et al., 2011), which may explain why it is difficult to identify nonessential assembly proteins for chloroplast ATP synthase. In this study, we developed a powerful strategy for isolating ATP synthase mutants. By monitoring NPQ levels within 2 min of illumination, we isolated several stable lines with reduced ATP synthase levels ranging from 25% to 75% of wild-type levels, indicating that our system is highly effective. We identified several mutants and found that all of the mutants had a defect in a gene that encodes the biogenesis factors specifically required for chloroplast ATP synthase. We thus designated these mutants the *bfa* mutants. We then isolated and characterized BFA3, a nucleus-encoded protein factor that is involved in the assembly of the CF_1 subcomplex of the chloroplast ATP synthase.

Loss of BFA3 in *bfa3* led to an approximately 75% reduction in chloroplast ATP synthase levels, whereas other thylakoid protein complexes were not affected (Fig. 3), indicating that the mutation in *bfa3* specifically affects the accumulation of chloroplast ATP synthase. Due to the reduced ATP synthase activity in *bfa3*, strong overacidification of the lumen occurs, which in turn triggers the formation of higher levels of NPQ and represses photosynthetic electron transport at the Cyt b_6f complex (Fig. 2). Similar photosynthetic properties were also observed in other mutants with low accumulation of chloroplast ATP synthase (Rott et al., 2011; Zoschke et al., 2012; Rühle et al., 2014; Fristedt et al., 2015; Mao et al., 2015). Therefore, the results of our immunoblot and spectroscopy analyses indicate that *bfa3* is a typical mutant with a specific impairment in ATP synthase accumulation.

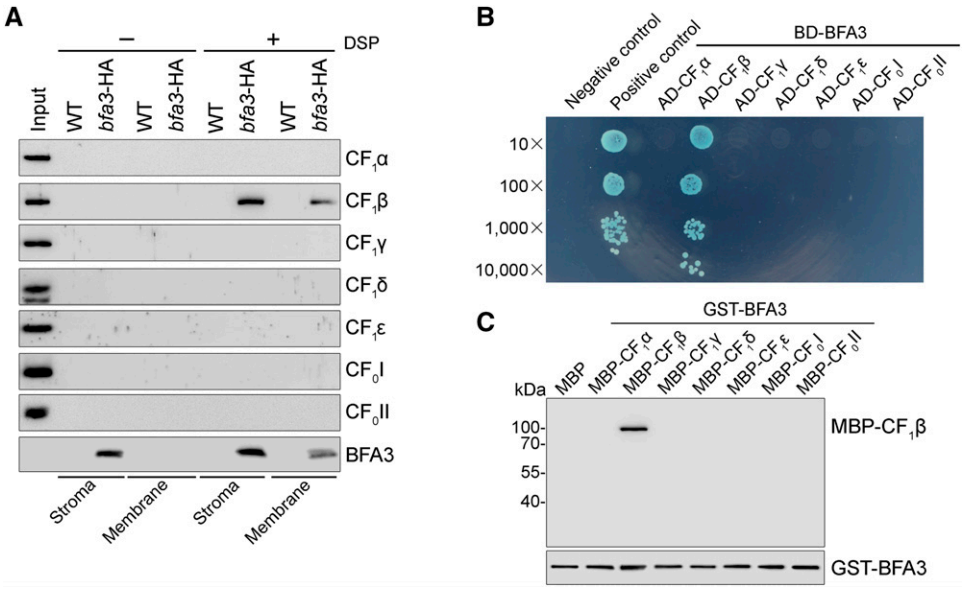

Figure 8. BFA3 specifically interacts with $CF_1\beta$. A, Affinity purification of the proteins associated with BFA3. Intact chloroplasts were isolated from leaves of WT and *bfa3*-HA plants and incubated with (+DSP) or without (-DSP) 2.5 mM DSP on ice for 30 min in the dark. After incubation, chloroplasts were osmotically ruptured and fractionated into stromal and thylakoid fractions. Peripheral thylakoid protein released from thylakoids by 1.2% Triton X-100 and stromal fractions were mixed with anti-HA affinity matrix for immunoprecipitation, respectively. The bound proteins were washed, eluted, and detected by immunoblot analysis using the indicated antibodies. *bfa3*-HA represents *bfa3-1* transformed with WT genomic *BFA3* fused to the sequence encoding the HA epitope-tag. Thylakoid proteins corresponding to 0.2 μg chlorophyll were loaded as indicators for antibodies. B, Yeast two-hybrid analysis. BFA3 was fused to the bait vector. Subunits of the CF_1 subcomplex as well as soluble parts of CF_0I and CF_0II were fused to the prey construct. Cotransformation of pGBKT7-53 with pGADT7-T was used as a positive control, whereas cotransformation of pGBK7-Lam with pGADT7-T was used as a negative control. As another negative control (Supplemental Fig. S4) included to rule out self-activation of the prey, pGBKT7 was cotransformed with pGADT7 harboring ATP synthase subunits. AD, GAL4 activation domain; BD, GAL4 DNA-binding domain. C, In vitro pull-down assay. GST-BFA3 fusion was used as bait. MBP-tagged $CF_1\alpha$, $CF_1\beta$, $CF_1\gamma$, $CF_1\delta$, and $CF_1\varepsilon$ subunits as well as the MBP-tagged soluble parts of CF_0I and CF_0II were used as prey. After incubation of bait and prey proteins for 1 h at 4°C, glutathione-agarose beads were added to precipitate the bait and bound prey proteins. The bound proteins were eluted and analyzed by immunoblotting with antibodies against MBP and BFA3.

The drastically reduced chloroplast ATP synthase levels in *bfa3* are not due to defects at the transcriptional and translational steps of ATP synthase gene expression. Inactivation of *BFA3* led to reduced *atpH/F* transcript levels but had no obvious effect on polysome loading of this transcript (Supplemental Fig. S1). Such moderate changes in the transcript accumulation of chloroplast ATP synthase genes are usually detected in other typical ATP synthase mutants. The maize *atp4* mutant and Arabidopsis *atcgl160* mutant exhibited reduced levels of *atpH/F* transcripts, but these mutations are not directly involved in the expression of *atpH/F* (Zoschke et al., 2012; 2013; Rühle et al., 2014; Fristedt et al., 2015). The reduced *atpH/F* transcript levels in these mutants suggest that an unknown regulatory mechanism may function at the transcriptional level, which is stimulated by low levels of chloroplast ATP synthase. It is also possible that the reduced *atpH/F* transcript levels may be a destabilization effect mediated by translational regulation. Such effects are also observed in the *petA* gene expression system in *Chlamydomonas* (Boulouis et al., 2011). Unlike its effects on *atpH/F*, loss of BFA3 resulted in a drastic increase in *atpB* transcript levels (Supplemental Fig. S1). This may represent a compensatory mechanism activated by the failure of $CF_1\beta$ assembly. An investigation of the regulation of CF_1 subcomplex biogenesis in *C. reinhardtii* (Drapier et al., 2007) showed that the stoichiometric accumulation of chloroplast-encoded ATP synthase subunits is controlled by the Control by Epistasy of Synthesis process at the translational level. It is currently unclear whether the Control by Epistasy of Synthesis process also occurs in higher plants. However, the altered transcript accumulation of ATP synthase genes in *bfa3*, as well as in other typical ATP synthase mutants, strongly suggests that the transcript levels of chloroplast-encoded ATP synthase genes are dynamically regulated.

Protein labeling and chase experiments provide direct evidence that BFA3 is involved in CF_1 subcomplex assembly (Figs. 4 and 6). This idea is consistent with the observation that BFA3 specifically interacts with the β-subunit of CF_1 (Figs. 8 and 9). BFA3 interacts with $CF_1\beta$ at the CS site; this region shows hydrophobic properties and has a strong tendency to aggregate (Ackerman, 2002). How does BFA3 promote the

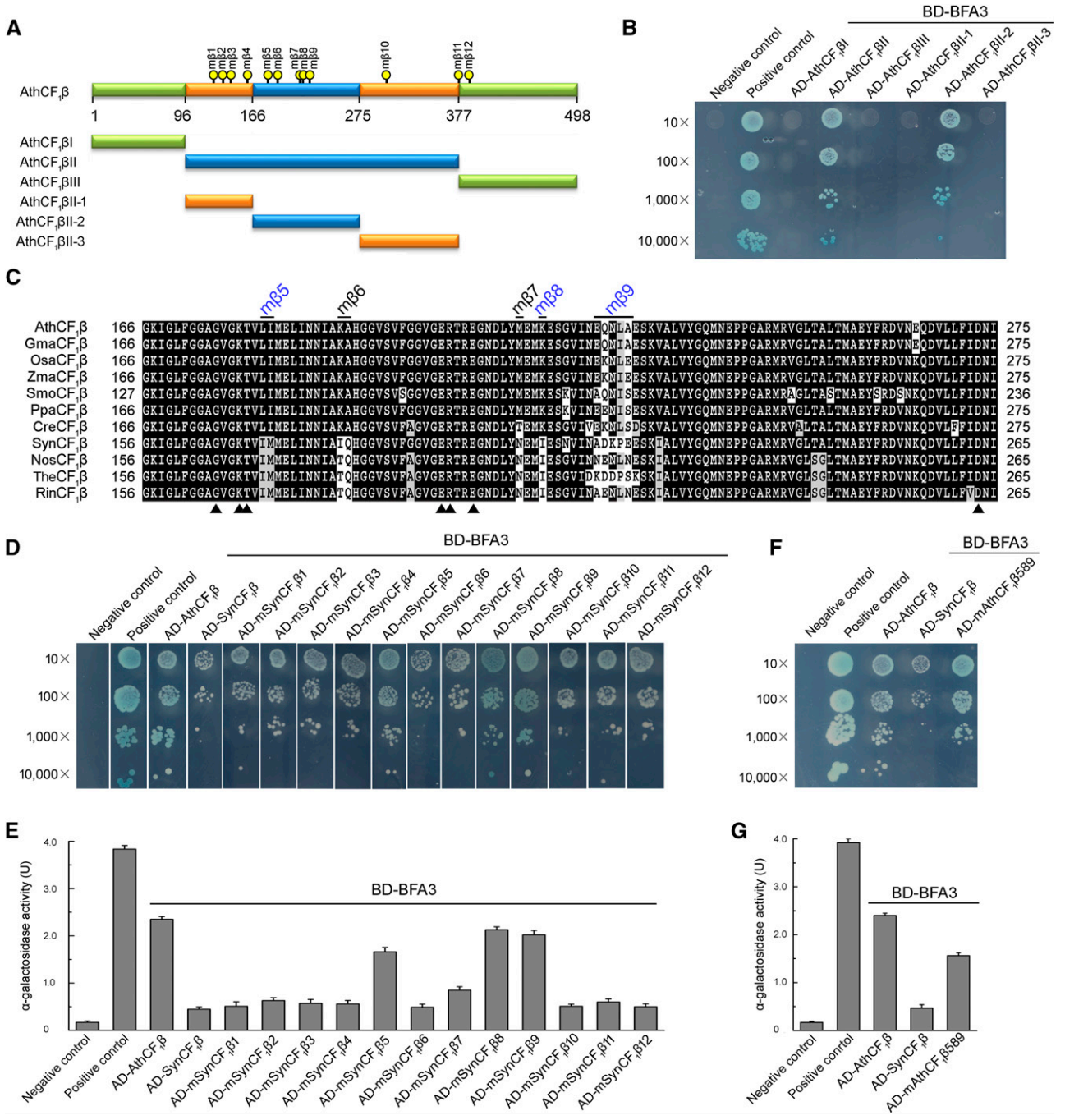

Figure 9. Mapping the critical residues of $CF_1\beta$ required for the interaction with BFA3. A, Diagram of $CF_1\beta$ and various deletions (I, II, III, II-1, II-2, and II-3) of $CF_1\beta$. The positions of the point mutation (mβ1-mβ12) are indicated by yellow dots. B, Yeast two-hybrid analysis of the interaction between BFA3 and various deletions of $AthCF_1\beta$. C, Amino acid sequence alignment of the interacting region ($AthCF_1\beta$II-2) corresponding to amino acid residues 166 to 275 in Arabidopsis $CF_1\beta$. The positions of the point mutation (mβ5-mβ9) are indicated. The residues for nucleotide binding in $CF_1\beta$ are indicated by closed triangles. Ath, Arabidopsis thaliana; Gma, *Glycine max*; Osa, *Oryza sativa*; Zma, *Zea mays*; Smo, *Selaginella moellendorffii*; Ppa, *Physcomitrella patens*; Cre, *Chlamydomonas reinhardtii*; Syn, *Synechocystis* sp. PCC 6803; Nos, *Nostoc* sp. PCC 7120; The, *Thermosynechococcus elongatus* BP-1; Rin, *Richelia intracellularis*. D, Yeast two-hybrid analysis of the interaction between BFA3 and $SynCF_1\beta$ variants. In these variants, the residues in $SynCF_1\beta$ were point mutated to the corresponding residues in $AthCF_1\beta$ and designated as $mSynCF_1\beta$1- $mSynCF_1\beta$12. E, Quantitative α-galactosidase assay. The strength of interaction was quantified by assaying α-galactosidase activity in yeast colonies using *p*-nitrophenyl α-D-galactopyranoside as substrate. Mean and SD of α-Gal activity were obtained from three independent colonies. F, Yeast two-hybrid analysis of the interaction between BFA3 and the $AthCF_1\beta$589 variant. In the $AthCF_1\beta$589 variant, the residues in $AthCF_1\beta$ at the positions of mβ5, mβ8, and mβ9 (A and C) were point mutated to the corresponding residues in $SynCF_1\beta$. G, Quantitative α-galactosidase assay performed as in E.

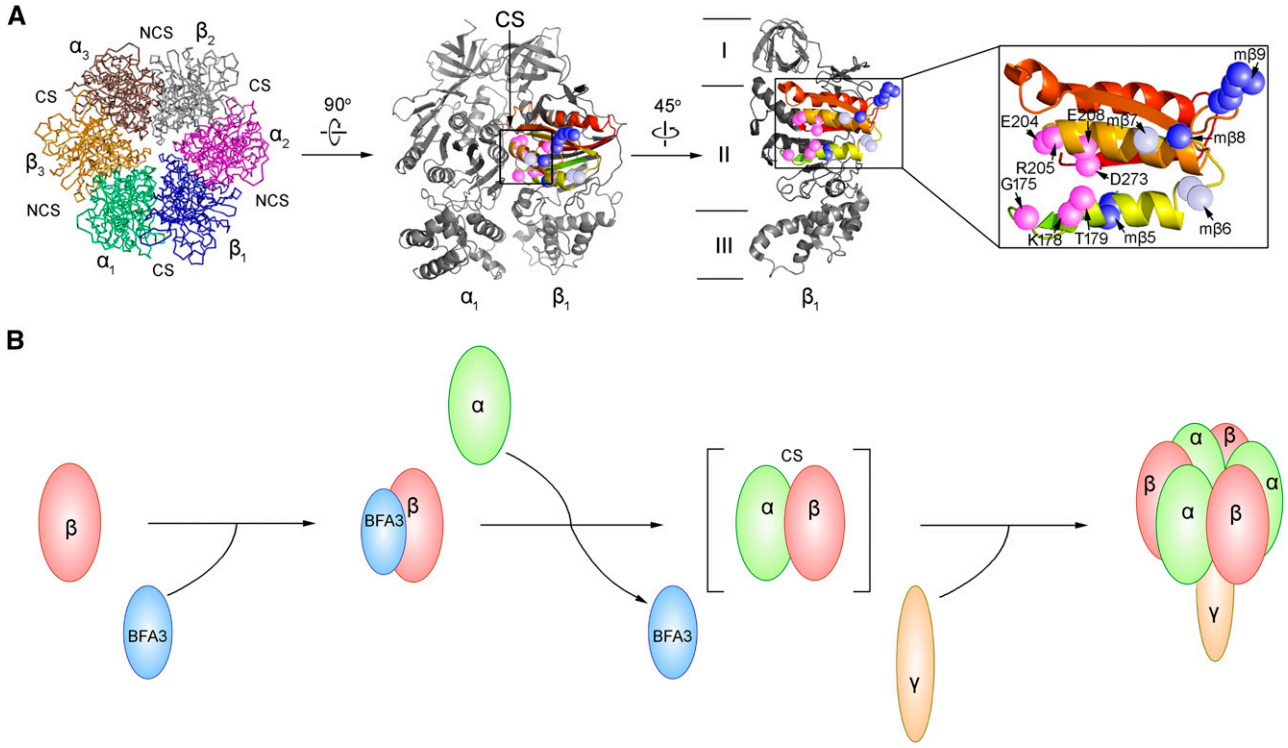

Figure 10. Model of the function of BFA3 during assembly of the CF_1 subcomplex. A, Top view of the $\alpha_3\beta_3$ hexamer and side view of the $\alpha\beta$ heterodimer. The interacting region $AthCF_1\beta II$-2 corresponding to amino acid residues 166 to 275 in Arabidopsis $CF_1\beta$ is shaded a range of colors (from lime to red) from the N to C terminal. Several residues (Leu-181-Ile-182, Met-217, and Glu-224-Ala-228 in $AthCF_1\beta$) critical for the interaction between BFA3 and $CF_1\beta$ are marked with blue spheres, whereas the residues in mβ6 and mβ7 are marked with gray spheres. Catalytic residues (Gly-175, Lys-178, Thr-179, Glu-204, Arg-205, Glu-208, and Asp-273) in $CF_1\beta$ are highlighted with pink spheres. B, Model of assembly of the $CF_1\alpha\beta$ complex. BFA3 directly interacts with the β-subunit and facilitates the assembly with the $CF_1\alpha$ subunit.

assembly of the CF_1 subcomplex? In mitochondria, Atp11p is an assembly factor that specifically interacts with the F1β subunit at the CS site and facilitates the assembly of the F1 subcomplex (Wang et al., 2000; Wang and Ackerman, 2000). Although Atp11p is believed to prevent aggregation of the unassembled β-subunit, its exact molecular role in F1 assembly is unclear (Ackerman and Tzagoloff, 2005). No homolog of *Atp11p* was found in the cyanobacterial genome, implying that assembly of cyanobacterial ATP synthase does not require Atp11p. Although an Atp11p-like protein (AT2G34050) was found in Arabidopsis, BFA3 does not share sequence similarity with this protein. Furthermore, we overexpressed AT2G34050 in the chloroplast with RbcS transit peptide, and the transformation failed to complement the phenotype of the *bfa3* mutants (data no shown). Thus, BFA3 and Atp11p likely play different roles during the assembly of ATP synthase, although they bind to the β-subunit at the same position. It is possible that, as a molecular chaperone, BFA3 transiently interacts with unassembled $CF_1\beta$ and that this type of interaction may not only prevent aggregation of β:β complex but also induce some conformational change in the $CF_1\beta$ subunit, thus promoting subsequent interaction between $CF_1\beta$ and $CF_1\alpha$ to form α:β intermediates (Fig. 10B).

BFA3 is conserved in higher plants, green algae, and a few species of other eukaryotic algae. No homologous protein was found in other eukaryotic algae or in any of the prokaryotic algae (Supplemental Fig. S2; Supplemental Table S1), implying that BFA3 was acquired by Viridiplantae (land plants and green algae) during evolution. Cursory examination of the critical $CF_1\beta$ residues for BFA3 binding (Supplemental Table S1) showed the following: (1) For residues in $CF_1\beta$5, 181Leu-182Ile (LI) are strictly conserved in all of the photosynthetic eukaryotes and two species of prokaryotic algae (Prochlorophyta). The corresponding residues in most species of prokaryotic algae are Ile-Met. We examined more than 200 species of prokaryotic algae and found that only three species have different residues in $CF_1\beta$5 (Ile-Ile). (2) For residue in $CF_1\beta$8, 217Lys (K) is highly conserved in photosynthetic eukaryotes and six species of prokaryotic algae (6 of more than 200 species). The corresponding residue in $CF_1\beta$8 in most prokaryotic algae is Ile (I) or Met (M). (3) The residues in $CF_1\beta$9 (224Glu-228Ala) are quite variable. However, there is still an evolutionary tendency for some residues to be conserved. For example, the first residue is Glu (E) in most of the photosynthetic eukaryotes but different in most of the prokaryotic

algae (Supplemental Table S1). From these results, we concluded that evolution of the critical $CF_1\beta$ residues for BFA3 binding occurred prior to the appearance of BFA3 in Viridiplantae.

It is currently unclear why the $CF_1\beta$ subunit would have undergone this type of evolution so that chloroplasts must recruit an assembly factor, BFA3, to facilitate the assembly of $CF_1\beta$. ATP synthase activity is regulated at several levels, including activity inhibition by Mg-ADP at the catalytic nucleotide-binding site (Fitin et al., 1979), activity inhibition by subunit ε (Patrie and McCarty, 1984), and activity modulation by oxidation/reduction of two Cys residues in the γ-subunit (Nalin and McCarty, 1984). Redox-regulation of ATP synthase activity via the γ-subunit only occurs in higher plants and green algae (Miki et al., 1988), suggesting that the regulatory mechanism of ATP synthase activity is quite different between cyanobacteria and photosynthetic eukaryotes (Ort and Oxborough, 1992). Based on the structure of $CF_1\beta$, it is clear that the residues in $CF_1\beta5$ are very close to the ADP/ATP binding site. Although the residue in $CF_1\beta8$ is relatively far from the CS site, it localizes to the same helix with ADP/ATP binding residues, including E204, R205, and E208. The residues in $CF_1\beta9$ are far from CS site. Given that the critical $CF_1\beta$ residues for BFA3 binding, especially the residues in $CF_1\beta5$ and $CF_1\beta8$, are located very close to the catalytic nucleotide binding site (Fig. 10A), it is possible that the structural alteration in the critical $CF_1\beta$ residues for BFA3 binding in eukaryotic $CF_1\beta$ enhances the regulatory activity of this subunit by increasing the efficiency of binding/release of Mg-ADP compared to its counterparts in cyanobacteria. This type of evolutionary function, together with other regulatory strategies acquired in photosynthetic eukaryotes, may allow ATP synthase activity to be fine-tuned in response to changes in environmental conditions specific to chloroplasts.

MATERIALS AND METHODS

Plant Material and Growth Conditions

Arabidopsis (*Arabidopsis thaliana*) plants were grown in potting soil under controlled greenhouse conditions (50 μmol photons m^{-2} s^{-1}, 16-h photoperiod, 23°C). Mutant screening was performed using the Closed FluorCam FC 800-C (Photon Systems Instruments) from sets of pools of pSKI015 T-DNA insertion Arabidopsis lines (stock no.: CS31400) obtained from the Arabidopsis Biological Resource Center. Digital images of chlorophyll fluorescence were recorded immediately before and during each saturating pulse using the MAXI version of an IMAGING PAM fluorometer (Walz, Effeltrich, Germany). Images of Chl fluorescence parameters were extracted using the software provided by the manufacturer (Imaging Win, Walz). The T-DNA insertion lines *bfa3-1* (SALK_019326) and *bfa3-2* (SALK_006444C) were obtained from NASC. Because the ecotype of *bfa3-3* is C24, we use *bfa3-1* and *bfa3-2* (ecotype of both mutants is Col-0) for most of the experiments.

Chlorophyll Fluorescence and P700 Analysis

The typical trace of chlorophyll fluorescence was monitored as previously described (Shikanai et al., 1999), except that measurements were performed in the dark. During illumination, saturating pulses of white light (0.8 s, 6000 μmol photons m^{-2} s^{-1}) were applied every 30 s to determine the maximum chlorophyll fluorescence in the light (F_m'). NPQ, ETR, and 1-qL were measured as previously reported (Miyake et al., 2009; Yamamoto et al., 2011). Light intensity-dependent oxidation of the donor side of PSI was measured using Dual-PAM-100 (Walz) and calculated automatically with Dual-PAM-100 software. The maximal P700 signal, P_m, was determined by applying a saturating pulse (6000 μmol photons m^{-2} s^{-1} for 0.8 ms) in the presence of far red light. During subsequent illumination (illumination for 3 min for each light intensity), saturating pulses were applied to determine the maximum $P700^+$ absorption under illumination (Pm).

pmf and ATP Synthase Activity Measurements

The pmf and its two components ($\Delta\Psi$ and ΔpH) were measured using a Dual-PAM-100 equipped with a P515/535 emitter-detector module (Walz; Schreiber and Klughammer, 2008). The measurement was carried out at 23°C under ambient CO_2 conditions (380 ppm, supplied with a GFS-3000 gas exchange measuring system). Plants were dark-adapted overnight, and detached leaves were illuminated for 10 min with 89 or 754 μmol photons m^{-2} s^{-1} red light. After illumination, inverse electrochromic band-shift kinetics was recorded for 2 min. Values for pmf, $\Delta\Psi$, and ΔpH were calculated as described (Schreiber and Klughammer, 2008). Light-dependent ATP synthase activity was measured at various light intensities (95, 216, 339, 531, and 825 μmol photons m^{-2} s^{-1}) as described (Rott et al., 2011).

Subcellular Localization of GFP-Fusion Proteins

Full-length cDNA of *BFA3* was cloned into pBI221 to express the BFA3-GFP fusion protein. The constructs for chloroplast and mitochondria localization were produced as previously described (Zhong et al., 2013). Arabidopsis protoplasts were transformed with various constructs via polyethylene glycol-mediated transformation and examined by confocal microscopy (LSM 510 Meta; Zeiss).

Intact Chloroplast Isolation, Stromal Fraction and Thylakoid Membrane Preparation, BN-PAGE, CN-PAGE, and Immunoblot Analysis

Intact chloroplasts were isolated and osmotically ruptured in buffer containing 20 mM HEPES-KOH, pH 7.6. The stromal fraction was separated from the membrane fraction by two rounds of centrifugation (15,000 g for 10 min at 4°C). Stromal protein concentrations were determined with a Protein Assay Kit (Bio-Rad), and chlorophyll contents were determined as described by Porra et al. (1989). Subsequent BN-PAGE, CN-PAGE, and immunoblot analysis were performed as described by Peltier et al. (2004).

Nucleic Acid Analysis

Total RNA was extracted from Arabidopsis leaves using Trizol reagent (Invitrogen). RT-PCR analysis was performed with a Scientific RevertAid First Strand cDNA Synthesis Kit (Thermo). RNA gel-blot analysis was performed using the DIG Easy Hyb system (Roche). Polysome association analysis was performed as described by Barkan (1988). The signals were visualized with a LuminoGraph WSE-6100 (ATTO). RL 6,000 RNA markers (Takara) were used as molecular markers.

In Vivo Labeling and Chasing of Chloroplast Proteins

Chloroplast protein labeling and chasing were performed as previously described (Meurer et al., 1998), with the following modifications. Primary leaves of 12-d-old young seedlings were preincubated in buffer containing 20 mg/ml cycloheximide for 30 min and radiolabeled with 1 mCi/mL [^{35}S]-Met in the presence of cycloheximide for 20 min at 80 μmol photons m^{-2} s^{-1} light intensity. After labeling, the leaves were washed and further incubated in buffer containing 1 mM unlabeled Met and 20 mg/mL cycloheximide for various periods of time. For membrane and soluble protein isolation, the labeled leaves were washed twice with a buffer containing 20 mM HEPES-KOH, pH 7.6, and ground with a conical plastic rod in a 1.5-mL tube with 20 μL of the same buffer. Soluble proteins were separated from the membranes by two rounds of centrifugation at 15,000 g for 10 min at 4°C.

Generation of Antibody against BFA3

Recombinant mature BFA3 protein was expressed in *Escherichia coli* BL21 (DE3) LysS strain and purified under denaturing conditions on a Ni-NTA agarose resin matrix. Polyclonal antibody was raised in rabbits with purified protein.

Yeast Two-Hybrid Assays

The Matchmaker Gold Yeast Two-hybrid System (Clontech) was used for the yeast two-hybrid assays. The sequence encoding mature BFA3 was cloned into pGBKT7 (DNA-binding domain) and used as bait. The coding sequences of $CF_1\alpha$, $CF_1\beta$, $CF_1\gamma$, $CF_1\delta$, and $CF_1\varepsilon$ subunits as well as the soluble parts of CF_0I and CF_0II were subcloned into pGADT7 (activation domain) and used as prey. The small-scale lithium acetate method was used to transform the Yeast strain Y2HGold. Control experiments were performed via cotransformation of positive and negative control plasmids. Positive colonies grown on double selection medium (SD/-Leu/-Trp) were cultured on SD/-Leu/-Trp/-His/-ade/X-α-Gal in the presence of aureobasidin A (50 ng/mL, Clontech) to investigate protein–protein interactions. The α-Gal quantitative assay was performed following the manufacturer's instructions (Clontech). Briefly, yeast cells were cultured in SD/-Leu/-Trp/-His medium to OD_{600} 0.5 to 1 and pelleted by centrifugation at 14,000 rpm. Then, 8 μL of supernatant was mixed with 24 μL of assay buffer (0.33 M sodium acetate, pH 4.5, and 33 mM *p*-nitrophenyl-α-D-galactopyranoside [Sigma]). After incubation at 30°C for 60 min, 960 μL of 0.1 M Na_2CO_3 was added to stop the reaction. The α-galactosidase activity was calculated as the optical density recorded at 410 nm.

Site-Directed Mutagenesis Vector Construction

PCR was performed using KOD Plus (ToYoBo) with pEASY-*SynATPB* or pEASY-*AthATPB* as the template. The primers are listed in Supplemental Table S2. After 15 cycles of PCR amplification at 95°C for 30 s, 56°C for 1 min, and 68°C for 10 min in a thermal cycler, the products were digested with *Dpn*I for 3 h at 37°C, and 5 μL of the reaction was used to transform *E. coli* DH5α competent cells. The resulting vectors were confirmed by DNA sequence analysis, and the mutated fragments were cloned into pGADT7.

Cross-Linking, Affinity Chromatography, and Pull-Down Analysis

Intact chloroplasts were suspended in a buffer containing 0.33 M sorbitol and 20 mM HEPES-KOH, pH 7.6 (0.5 mg chlorophyll/mL), and cross-linked with 2.5 mM DSP. After incubation for 30 min on ice in darkness, 1 M Tris-HCl, pH 7.5, was added to a final concentration of 60 mM to stop the reaction. Chloroplasts were osmotically ruptured with 20 mM HEPES-KOH (pH 7.6). Thylakoids were pelleted by centrifugation, and the supernatant stromal fraction was transferred to new tubes and mixed with Anti-HA Affinity Matrix (Roche). Thylakoid membrane was solubilized for 30 min at 4°C in a buffer containing 20 mM HEPES-KOH, pH 8.0, 1.2% Triton X-100, 200 mM NaCl, and 1 mM phenylmethylsulfonyl fluoride. After solubilization, insoluble thylakoids were removed by centrifugation, and the supernatant was mixed with Anti-HA Affinity Matrix. After incubation for 2 h at 4°C, the bound proteins were purified and detected with specific antibodies.

For pull-down assays, BFA3-GST, $CF_1\alpha$-MBP, $CF_1\beta$-MBP, $CF_1\gamma$-MBP, $CF_1\delta$-MBP, $CF_1\varepsilon$-MBP, CF_0I-MBP, CF_0II-MBP, and MBP were induced in *E. coli* BL21 (DE3) LysS strain by 0.3 mm isopropyl β-D-1-thiogalactopyranoside treatment at 16°C and purified using glutathione-agarose 4B beads (GE Healthcare) and amylose resin (New England Biolabs), respectively. Briefly, 5 μg of purified recombinant GST-BFA3 and 5 μg of MBP fusion or MBP proteins were incubated in 1 mL pull-down buffer (50 mM Tris-HCl, pH 7.5, 0.15 M NaCl, 1% Triton X-100, 5% glycerol, 1 mM dithiothreitol, and Complete protease inhibitor cocktail [Roche]) for 1 h at 4°C with end-over-end mixing. After incubation, 25 μL of glutathione-agarose beads was added to precipitate the bait and bound prey proteins. The bound proteins were eluted in SDS-PAGE sample buffer and analyzed by immunoblotting.

Accession Numbers

Sequence data from this article can be found in the Arabidopsis Genome Initiative or GenBank/EMBL databases under the following accession numbers: AtBFA3 (AT2G21385, Arabidopsis), GmBFA3 (XP_006592087.1, *Glycine max*), OsBFA3 (XP_015611535.1, *Oryza sativa*), ZmBFA3 (ACG43670.1, *Zea mays*), SmBFA3 (XP_002964112.1, *Selaginella moellendorffii*), PpBFA3 (XP_001780245.1, *Physcomitrella patens*) and CrBFA3 (XP_001701296.1, *Chlamydomonas reinhardtii*). Ath$CF_1\beta$ (ATCG00480, Arabidopsis thaliana), Gma$CF_1\beta$ (YP_538748.1, *Glycine max*), Osa$CF_1\beta$ (YP_052756.1, *Oryza sativa*), Zma$CF_1\beta$ (NP_043032.1, *Zea mays*), Smo$CF_1\beta$ (YP_003097494.1, *Selaginella moellendorffii*), Ppa$CF_1\beta$ (NP_904195.1, *Physcomitrella patens*), Cre$CF_1\beta$ (NP_958414.1, *Chlamydomonas reinhardtii*), Syn $CF_1\beta$ (WP_010872712.1, *Synechocystis* sp. PCC 6803), Nos$CF_1\beta$ (WP_010999165.1, *Nostoc* sp. PCC 7120), The$CF_1\beta$ (NP_681315.1, *Thermosynechococcus elongatus* BP-1), Rin$CF_1\beta$ (CDN15135.1, *Richelia intracellularis*).

Supplemental Data

The following supplemental materials are available.

Supplemental Figure S1. RNA gel-blot and polysome analysis.

Supplemental Figure S2. Alignment of BFA3 homologs.

Supplemental Figure S3. Suc density gradient analysis of stromal proteins.

Supplemental Figure S4. Control for yeast two-hybrid analysis.

Supplemental Figure S5. Alignment of $CF_1\beta$ protein sequences.

Supplemental Table S1. Phylogenetic analysis of BFA3 and CF1β.

Supplemental Table S2. Primers used in this work.

ACKNOWLEDGMENTS

We thank the Arabidopsis Biological Resource Center and NASC for providing the mutant seeds.

Received February 16, 2016; accepted April 12, 2016; published April 18, 2016.

LITERATURE CITED

Ackerman SH (2002) Atp11p and Atp12p are chaperones for $F(_1)$-ATPase biogenesis in mitochondria. Biochim Biophys Acta **1555:** 101–105

Ackerman SH, Tzagoloff A (2005) Function, structure, and biogenesis of mitochondrial ATP synthase. Prog Nucleic Acid Res Mol Biol **80:** 95–133

Bailleul B, Cardol P, Breyton C, Finazzi G (2010) Electrochromism: a useful probe to study algal photosynthesis. Photosynth Res **106:** 179–189

Barkan A (1988) Proteins encoded by a complex chloroplast transcription unit are each translated from both monocistronic and polycistronic mRNAs. EMBO J **7:** 2637–2644

Benz M, Bals T, Gügel IL, Piotrowski M, Kuhn A, Schünemann D, Soll J, Ankele E (2009) Alb4 of *Arabidopsis* promotes assembly and stabilization of a non chlorophyll-binding photosynthetic complex, the CF_1CF_0-ATP synthase. Mol Plant **2:** 1410–1424

Boulouis A, Raynaud C, Bujaldon S, Aznar A, Wollman FA, Choquet Y (2011) The nucleus-encoded *trans*-acting factor MCA1 plays a critical role in the regulation of cytochrome *f* synthesis in *Chlamydomonas* chloroplasts. Plant Cell **23:** 333–349

Chen GG, Jagendorf AT (1994) Chloroplast molecular chaperone-assisted refolding and reconstitution of an active multisubunit coupling factor CF1 core. Proc Natl Acad Sci USA **91:** 11497–11501

Choquet Y, Vallon O (2000) Synthesis, assembly and degradation of thylakoid membrane proteins. Biochimie **82:** 615–634

Cruz JA, Sacksteder CA, Kanazawa A, Kramer DM (2001) Contribution of electric field ($\Delta\Psi$) to steady-state transthylakoid proton motive force (pmf) *in vitro* and *in vivo*. Biochemistry **40:** 1226–1237

DalCorso G, Pesaresi P, Masiero S, Aseeva E, Schünemann D, Finazzi G, Joliot P, Barbato R, Leister D (2008) A complex containing PGRL1 and PGR5 is involved in the switch between linear and cyclic electron flow in *Arabidopsis*. Cell **132:** 273–285

Drapier D, Rimbault B, Vallon O, Wollman FA, Choquet Y (2007) Intertwined translational regulations set uneven stoichiometry of chloroplast ATP synthase subunits. EMBO J **26:** 3581–3591

Fitin AF, Vasilyeva EA, Vinogradov AD (1979) An inhibitory high affinity binding site for ADP in the oligomycin-sensitive ATPase of beef heart submitochondrial particles. Biochem Biophys Res Commun **86:** 434–439

Foyer C, Furbank R, Harbinson J, Horton P (1990) The mechanisms contributing to photosynthetic control of electron transport by carbon assimilation in leaves. Photosynth Res **25:** 83–100

Fristedt R, Martins NF, Strenkert D, Clarke CA, Suchoszek M, Thiele W, Schöttler MA, Merchant SS (2015) The thylakoid membrane protein CGL160 supports CF_1CF_0 ATP synthase accumulation in *Arabidopsis thaliana*. PLoS One **10:** e0121658

Groth G, Pohl E (2001) The structure of the chloroplast F_1-ATPase at 3.2 A resolution. J Biol Chem **276:** 1345–1352

Hippler M, Rimbault B, Takahashi Y (2002) Photosynthetic complex assembly in *Chlamydomonas reinhardtii.* Protist **153:** 197–220

Junge W, Nelson N (2015) ATP synthase. Annu Rev Biochem **84:** 631–657

Kanazawa A, Kramer DM (2002) In vivo modulation of nonphotochemical exciton quenching (NPQ) by regulation of the chloroplast ATP synthase. Proc Natl Acad Sci USA **99:** 12789–12794

Malik Ghulam M, Zghidi-Abouzid O, Lambert E, Lerbs-Mache S, Merendino L (2012) Transcriptional organization of the large and the small ATP synthase operons, *atpI/H/F/A* and *atpB/E*, in *Arabidopsis thaliana* chloroplasts. Plant Mol Biol **79:** 259–272

Mao J, Chi W, Ouyang M, He B, Chen F, Zhang L (2015) PAB is an assembly chaperone that functions downstream of chaperonin 60 in the assembly of chloroplast ATP synthase coupling factor 1. Proc Natl Acad Sci USA **112:** 4152–4157

Meurer J, Plücken H, Kowallik KV, Westhoff P (1998) A nuclear-encoded protein of prokaryotic origin is essential for the stability of photosystem II in *Arabidopsis thaliana.* EMBO J **17:** 5286–5297

Miki J, Maeda M, Mukohata Y, Futai M (1988) The γ-subunit of ATP synthase from spinach chloroplasts. Primary structure deduced from the cloned cDNA sequence. FEBS Lett **232:** 221–226

Miyake C, Amako K, Shiraishi N, Sugimoto T (2009) Acclimation of tobacco leaves to high light intensity drives the plastoquinone oxidation system–relationship among the fraction of open PSII centers, nonphotochemical quenching of Chl fluorescence and the maximum quantum yield of PSII in the dark. Plant Cell Physiol **50:** 730–743

Munekage Y, Hojo M, Meurer J, Endo T, Tasaka M, Shikanai T (2002) PGR5 is involved in cyclic electron flow around photosystem I and is essential for photoprotection in *Arabidopsis*. Cell **110:** 361–371

Nalin CM, McCarty RE (1984) Role of a disulfide bond in the γ subunit in activation of the ATPase of chloroplast coupling factor 1. J Biol Chem **259:** 7275–7280

Niyogi KK (1999) Photoprotection revisited: genetic and molecular approaches. Annu Rev Plant Physiol Plant Mol Biol **50:** 333–359

Ort DR, Oxborough K (1992) In situ regulation of chloroplast coupling factor activity. Annu Rev Plant Biol **43:** 269–291

Patrie WJ, McCarty RE (1984) Specific binding of coupling factor 1 lacking the δ and ε subunits to thylakoids. J Biol Chem **259:** 11121–11128

Peltier JB, Ripoll DR, Friso G, Rudella A, Cai Y, Ytterberg J, Giacomelli L, Pillardy J, van Wijk KJ (2004) Clp protease complexes from photosynthetic and non-photosynthetic plastids and mitochondria of plants, their predicted three-dimensional structures, and functional implications. J Biol Chem **279:** 4768–4781

Porra RJ, Thompson WA, Kriedemann PE (1989) Determination of accurate extinction coefficients and simultaneous equations for assaying chlorophylls *a* and *b* extracted with four different solvents: verification of the concentration of chlorophyll standards by atomic absorption spectrometry. Biochim Biophys Acta **975:** 384–394

Rak M, Gokova S, Tzagoloff A (2011) Modular assembly of yeast mitochondrial ATP synthase. EMBO J **30:** 920–930

Rott M, Martins NF, Thiele W, Lein W, Bock R, Kramer DM, Schöttler MA (2011) ATP synthase repression in tobacco restricts photosynthetic electron transport, CO_2 assimilation, and plant growth by overacidification of the thylakoid lumen. Plant Cell **23:** 304–321

Rühle T, Leister D (2015) Assembly of F_1F_0-ATP synthases. Biochim Biophys Acta **1847:** 849–860

Rühle T, Razeghi JA, Vamvaka E, Viola S, Gandini C, Kleine T, Schünemann D, Barbato R, Jahns P, Leister D (2014) The Arabidopsis protein CONSERVED ONLY IN THE GREEN LINEAGE160 promotes the assembly of the membranous part of the chloroplast ATP synthase. Plant Physiol **165:** 207–226

Schreiber U, Klughammer C (2008) New accessory for the Dual-PAM-100: the P515/535 module and examples of its application. PAN **1:** 1–10

Shikanai T, Munekage Y, Shimizu K, Endo T, Hashimoto T (1999) Identification and characterization of *Arabidopsis* mutants with reduced quenching of chlorophyll fluorescence. Plant Cell Physiol **40:** 1134–1142

Strotmann H, Shavit N, Leu S (1998) Assembly and function of the chloroplast ATP synthase. The molecular biology of chloroplast and mitochondria in *Chlamydomonas*. JD Rochaix, M Goldschmidt-Clermont, and S Merchant, eds. Kluwer Academic Publishers, Norwell, MA, pp 477–500

von Ballmoos C, Wiedenmann A, Dimroth P (2009) Essentials for ATP synthesis by F_1F_0 ATP synthases. Annu Rev Biochem **78:** 649–672

Vollmar M, Schlieper D, Winn M, Büchner C, Groth G (2009) Structure of the c_{14} rotor ring of the proton translocating chloroplast ATP synthase. J Biol Chem **284:** 18228–18235

Wang ZG, Ackerman SH (2000) The assembly factor Atp11p binds to the β-subunit of the mitochondrial $F_{(1)}$-ATPase. J Biol Chem **275:** 5767–5772

Wang ZG, Sheluho D, Gatti DL, Ackerman SH (2000) The α-subunit of the mitochondrial $F_{(1)}$ ATPase interacts directly with the assembly factor Atp12p. EMBO J **19:** 1486–1493

Weber J (2007) ATP synthase–the structure of the stator stalk. Trends Biochem Sci **32:** 53–56

Wollman FA, Minai L, Nechushtai R (1999) The biogenesis and assembly of photosynthetic proteins in thylakoid membranes1. Biochim Biophys Acta **1411:** 21–85

Yamamoto H, Peng L, Fukao Y, Shikanai T (2011) An Src homology 3 domain-like fold protein forms a ferredoxin binding site for the chloroplast NADH dehydrogenase-like complex in *Arabidopsis*. Plant Cell **23:** 1480–1493

Yoshida M, Muneyuki E, Hisabori T (2001) ATP synthase–a marvellous rotary engine of the cell. Nat Rev Mol Cell Biol **2:** 669–677

Zhong L, Zhou W, Wang H, Ding S, Lu Q, Wen X, Peng L, Zhang L, Lu C (2013) Chloroplast small heat shock protein HSP21 interacts with plastid nucleoid protein pTAC5 and is essential for chloroplast development in *Arabidopsis* under heat stress. Plant Cell **25:** 2925–2943

Zoschke R, Kroeger T, Belcher S, Schöttler MA, Barkan A, Schmitz-Linneweber C (2012) The pentatricopeptide repeat-SMR protein ATP4 promotes translation of the chloroplast *atpB/E* mRNA. Plant J **72:** 547–558

Zoschke R, Qu Y, Zubo YO, Börner T, Schmitz-Linneweber C (2013) Mutation of the pentatricopeptide repeat-SMR protein SVR7 impairs accumulation and translation of chloroplast ATP synthase subunits in *Arabidopsis thaliana.* J Plant Res **126:** 403–414